ELSEVIER

Docking of sulfonamides to carbonic anhydrase II and IV

Emilio Xavier Esposito,* Kelli Baran,* Ken Kelly,† and Jeffry D. Madura*

**Department of Chemistry and Biochemistry, Duquesne University, Pittsburgh, Pennsylvania, USA*
†Chemical Computing Group Inc., Montreal, Quebec, Canada

Starting with a known active site of a protein and a database of compounds, one would like to quickly identify a few compounds that "dock" into the active site and obtain "good" binding free energies. The main goal of current automated docking procedures is to predict the "best" substrate–enzyme complex while other programs such as UHBD and DelPhi can be used to compute binding free energies. In this paper, we will focus on the application of docking methods and parameters to study substrate–enzyme interactions of a metalloenzyme system. Specifically, we report on the docking of sulfonamides to carbonic anhydrase II and IV, which are of interest due to their application in glaucoma therapy. Using a standard docking protocol, it is possible to correctly predict not only the orientation of inhibitors to a specific isozyme, but also determine the qualitative affinity for a group of inhibitors for an isozyme. © 2000 by Elsevier Science Inc.

Keywords: docking, metalloenzymes, carbonic anhydrase, molecular operating environment

*Abbreviations CA, carbonic anhydrase; IE, interaction energy; IOP, intraocular pressure; MOE, molecular operating environment; ESP, electrostatic potential; RMSD, root mean squared deviation; IN3R, (*R*)-3,4-dihydro-2-(3-methoxyphenyl)-4-methyl-amino-2H-thienol[3,2-e]-1,2-thiazine-6-sulfonamide-1,1-dioxide; AZP, (*R*)-4-ethylamino-3,4-dihydro-2-(3-methoxy)propyl-2H-thieno[3,2-e]-1,2-thiazine-6-sulfonamide-1,1-dioxide; IN2R, (*R*)-4-ethylamino-3,4-dihydro-2-(2-methoxy)propyl-2H-thieno[3,2-e]-1,2-thiazine-6-sulfonamide-1,1-dioxide; AMS, 4-aminobenzenesulfonamide; IN3S, (*S*)-3,4-dihydro-2-(3-methoxyphenyl)-4-methyl-amino-2H-thienol[3,2-e]-1,2-thiazine-6-sulfonamide-1,1-dioxide.*

Color plates for this article are on pages 307–308.

Corresponding author: J.D. Madura, Department of Chemistry and Biochemistry, Duquesne University, Pittsburgh, PA 15219, USA. Tel.: 412-396-4129; fax: 412-396-5683.

E-mail address: madura@duq.edu (J.D. Madura)

INTRODUCTION

Recent advances in protein structure determination, via X-ray crystallography, nuclear magnetic resonance, or computer models, are providing the necessary data for chemists, biochemists, and pharmacologists to design and study substrates/ligands for these proteins. Identifying the substrates that bind in the active site of these newly determined protein structures has led to the development of a variety of docking strategies.[1] In the case of enzymes, starting with a known active site and a database of compounds, it would be advantageous to be able to quickly identify a few compounds that "dock" into the active site and calculate "good" binding free energies. Most of these strategies have been developed using nonmetalloenzymes as case studies.[2–12]

There are various interactions between a substrate and receptor that must be modelled. Such interactions include shape complementarity, interaction specificity (charge–charge interactions), as well as solvation/desolvation interactions, hydrophobic interactions, and hydrogen bonding.[13,14] With the inclusion of each interaction, substrate–receptor complexes are better predicted; however, this comes at the expense of additional computational costs. To reduce computational costs, many of these interactions are either neglected or simplified. For example, the interaction energy (IE) between a substrate and an enzyme is calculated using a standard nonbonded 6-12 Lennard–Jones function and a Coulombic term. There are several well-documented force fields for proteins whose parameters can be used in docking calculations, yet most of these force fields do not have well-established parameters for metalloenzymes.[15–20]

Metalloenzymes are an important class of enzymes used to regulate CO_2 levels in the body, catalyze the conversion of fatty acids to amides, promote dioxygen and electron transport, and have roles in cellular structure composition.[21] In this paper, we will focus on the application of one particular docking method and the parameters used to study substrate–enzyme interactions of two isozymes of a single metalloenzyme system. Specifically, we report our efforts on the docking of sulfonamides to carbonic anhydrase (CA) II and IV. Recently, Boriack-Sjodin et al.[22] reported the specificity of CA II on

Journal of Molecular Graphics and Modelling 18, 283–289, 2000

655 Avenue of the Americas, New York, NY 10010

1093-3263/00/$–see front matter
PII S1093-3263(00)00040-1

different substrates, whereas Stams et al.[23] reported on the binding affinity of a specific substrate to two different isozymes, CA II and IV. These experimental results provide a good basis on which to evaluate the docking method and force field parameters used and the predicted substrate specificity

Seven different isozymes of the mammalian form of CA have been identified with distinct activities, tissue specificity, and physiological roles.[24,25] A high concentration of CA I is expressed in red blood cells, and CA II is dominant in the aqueous humor of the eye. CA III is present in the cytoplasm of muscle tissue cells. The only known mammalian membrane-bound isozyme is CA IV, which is bound to the membrane in the lung, kidney, brain, and eye. CA V is expressed in mitochondria, whereas isozymes CA VI and VII are detected in saliva and salivary glands.[25]

CA II and CA IV, both highly active CA isozymes, catalyze bicarbonate ion (HCO_3^-) formation in the aqueous humor, regulating intraocular pressure (IOP).[26] Immunochemical studies have determined that CA II is the most abundant isozyme of CA distributed in the eye, with high concentrations found in epithelial cells of the ciliary process, Müller cells of the retina, and a subset of cone photoreceptor cells.[24] Immunostaining determined that CA IV is located in the endothelial cells of the choriocapillaris. Further investigations found CA IV is expressed on the exterior surface of the plasma membrane on both the apical and basolateral surfaces of the epithelial cells.[24]

The main secondary structural difference between CA II and CA IV is the region of residues 130–140, which are approximately 6 to 8 Å from the active site. In human CA II, this region is a three-turn α-helix, whereas in human CA IV the region is a loop. This loop is believed to hold CA IV to the membrane of the cell.[23] The active site of CA is a conically shaped cleft, 15 Å in depth with an entrance approximately 15 Å wide. At the bottom of the active site near the apex of the cone is a zinc metal ion with a +2 charge. The location of the zinc ion is approximately at the center of the enzyme and is coordinated to the imidazole group of three histidines, His-94, His-96, and His-119, forming the base of a tetrahedron. The fourth zinc coordination site interacts with a hydroxide or the ligand.

Inhibitor Affinity

It was determined by Stams et al.[23] that the affinity of CA II for sulfonamide inhibitors is up to a 100 times more than CA IV. When bound, the ionized sulfonamide nitrogen, 1−, displaces a zinc-bound hydroxide, from the fore mentioned fourth zinc coordination site, to form a stable inhibitor–enzyme complex with nanomolar affinity.[22,23,26–33] The sulfonamide group of the inhibitor interacts with the zinc ion and the OH and NH groups of amino acid Thr-199.[27] The analogous susceptibility to aryl sulfonamide inhibition of CA II and CA IV makes aryl sulfonamides of interest in glaucoma therapy as an effective method to regulate IOP. Therefore, we selected five inhibitors, with a range of binding affinities (0.1–750 nM) (Table 1). 4-Aminobenzenesulfonamide (AMS) binds preferentially to CA II, whereas *(R)*-4-ethylamino-3,4-dihydro-2-(3-methoxy)-propyl-2H-thieno[3,2-e]-1,2-thiazine-6-sulfonamide-1,1-dioxide (AZP) preferentially binds to CA IV.

Docking Algorithms

Docking programs belong to two classes, "direct" and "unbiased." Direct docking methods such as DOCK[6] have the advantage of speed, yet the disadvantage of making assumptions about the potential energy landscape to save computational time. Unbiased methods such as AutoDock®,[5] FTDOCK,[34] and MOE-Dock[35] make few assumptions about the potential energy landscape. Thus, they find final docked solutions that the direct method might have missed, at the expense of computation time. Here we report the use of MOE-Dock by Chemical Computing Group Inc.,[36] which is based on the program AutoDock® 2.4 by Art Olsen at Scripps Research Institute.[5] It should be noted that this is not a comparison between MOE-Dock and AutoDock®, although AutoDock® was used to test the validity of MOE-Dock. Although MOE-Dock and AutoDock are very similar, MOE-Dock has the advantage of being integrated with a graphical interface as well as with other modules, such as analysis, molecular mechanics, and molecular dynamics.

MOE-Dock

MOE-Dock utilizes a Monte Carlo simulated annealing process for docking a substrate into the active site of a macromolecule. The program constructs a three-dimensional grid surrounding the center of the docking site. A probe atom visits each grid point; where the IE, which includes dispersion-repulsion and hydrogen bonding interactions, is calculated and stored. Separate tables are calculated for each type of atom in the ligand. The completed grids of energies provide a lookup table for the rapid evaluation of interaction energies. A separate electrostatic potential grid is calculated, using a probe carrying a single positive charge. The IE is calculated using electrostatic and van der Waal's potential energy terms that have been sampled on a grid overlaying the docking box. The electrostatic IE for each atom in the ligand then may be obtained during the simulation as the product of the local value taken from the grid point and the partial charge on the atom. The van der Waal's parameters are a traditional 6–12 Lennard–Jones potential, and the electrostatic energy is the standard Coulombic form with the dielectric set to one. Finally, the energy is calculated using the parameters from AMBER 89. The grid is not required; it is only used as a speed-up mechanism to avoid pairwise atom nonbonded calculations for each ligand conformer.

Once the initialization phase is complete, the substrate is randomly placed in the docking box. MOE-Dock allows the substrate to search six spatial degrees of freedom, rotational, translational, and any number of torsional degrees of freedom during the actual docking simulation. However, MOE does not allow conformations where a portion of the substrate protrudes from the docking box; an energy of infinity is assigned when this occurs and the conformation is not accepted. AutoDock®, on the other hand, manipulates the substrate so it remains in the grid box; this does not prohibit atoms from leaving the box in AutoDock® but instead the atoms outside of the box are assigned an IE of zero.

A random perturbation is applied at each step and the IE is evaluated for the new location and conformation. The new state is either accepted or rejected probabilistically based on the annealing temperature of the system.[8] This probability depends on the energy and temperature of the cycle. At a high temperature cycle, many conformation states will be accepted,

Table 1. Inhibitors Used in the Predicted Docking of Inhibitors in CA II and CA IV

Name	Structure	Binding affinity (nM)	Label
(*R*)-3,4-dihydro-2-(3-methoxyphenyl)-4-methyl-amino-2H-thienol[3,4-3]-1,2-thiazine-6-sulfonamide-1,1-dioxide	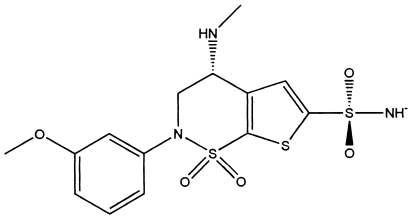	0.10 ± 0.01	IN3R
(*R*)-4-ethylamino-3,4-dihydro-2-(3-methoxy)propyl-2H-thieno[3,2-e]-1,2-thiazine-6-sulfonamide-1,1-dioxide	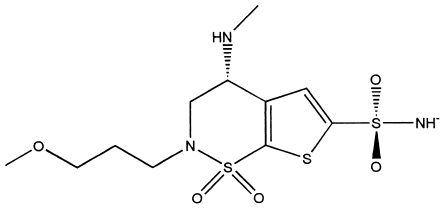	0.13 ± 0.03	AZP
(*R*)-4-ethylamino-3,4-dihydro-2-(2-methoxy)propyl-2H-thieno[3,2-e]-1,2-thiazine-6-sulfonamide-1,1-dioxide	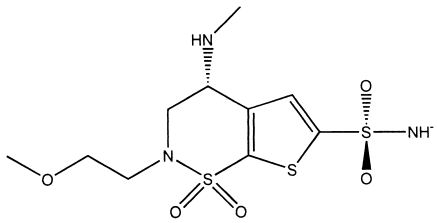	0.32 ± 0.05	IN2R
4-Aminobenzenesulfonamide	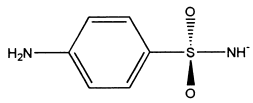	750	AMS
(*S*)-3,4-dihydro-2-(3-methoxyphenyl)-4-methyl-amino-2H-thienol[3,2-e]-1,2-thiazine-6-sulfonamide-1,1-dioxide	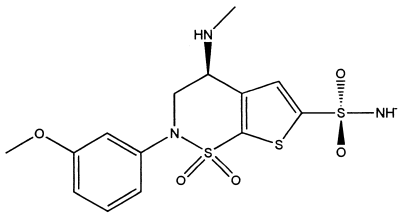	1.70 (single)	IN3S

whereas at a low temperature cycle, many of the low probabilistic states will be rejected. In principle, the global minimum eventually will be found on the potential energy surface. A typical docking calculation involves several cycles, comprised of 30,000–50,000 steps. The docked conformations are ranked according to interaction energies. The method of determining the "best" docked structure will be discussed later.

METHODS

In this paper, we used the X-ray structures of CA II (3ca2) with the bound inhibitor AMS to develop the docking protocol. This protocol was used on all other docking calculations. After all docking simulations were completed, Stams et al. provided us with the X-ray structures of AZP bound to CA II and IV for comparison of our theoretical results to their experimental results.

The edited PDB crystal structure (water molecules, AMS, and Hg atoms removed) of CA II (3ca2)[37,38] was imported into MOE and all possible hydrogen atoms were added. Three mercury atoms were used as positioning markers for the X-ray structure. Two mercury atoms were complexed to the enzyme and the third was bound to the aryl-ring of AMS. These mercury atoms had no significant effect on the structure of the enzyme. Atomic charges were assigned using the Kollman 89 force field parameters in MOE and the zinc metal ion was set to a +2 charge.

Considering that the active site of CA II (3ca2) might be biased to AMS, the inhibitors were docked into a native X-ray structure of CA II (1ca2),[38,39] which was not complexed with an inhibitor. 1ca2 was imported into MOE and hydrogen atoms added, Kollman 89 force fields assigned, and the zinc metal ion was set to a +2 charge. The backbone, zinc, and His-94, His-96, and His-119 were fixed and an energy minimization was performed. The energy minimization function in MOE uses a sequential combination of three different minimization techniques in each step of the minimization process. The first

technique is steepest descent[40] (100 iterations with an RMS gradient test limit of 1,000), which moves in the direction parallel to the net force, similar to walking down a hill in a path of least resistance. The next technique is the conjugate gradient[40] (100 iterations with an RMS gradient test of 100) where the gradients at each point are orthogonal but the direction is conjugate, whereas in the steepest descent method both the gradients and the direction of successive steps are orthogonal. The third minimization technique is a truncated Newton[40] (200 iterations with an RMS gradient of 0.01), which eliminates the off-diagonal elements for large distance interactions between atoms.

Starting coordinates for CA IV were obtained from the PDB crystal structure 1znc.[38,41] Chain B, SO_4^{2-}, and water molecules were removed from the PDB file. Chain B is the crystallographic dimer and CA IV functions as a monomer. The waters were removed from both enzymes because they would be fixed and therefore hinder the docking of the substrates. Once imported into MOE, hydrogen atoms were added and Kollman 89 force field charges assigned to the receptor. Again, the zinc metal ion was set to a +2 charge. Originally, the side chains of the CA IV active site were oriented toward the bound SO_4^{2-}; constricting the active site. Removal of the SO_4^{2-} from the active site allows the side chains in the active site to interact more with each other and produce a more "open" receptor. To "open" the active site, the backbone, zinc, and His-94, His-96, and His-119 were fixed and an energy minimization was performed. This "opened" structure then was used in MOE-Dock as the CA IV receptor. Because the docking calculations included electrostatic interactions, partial charges on the inhibitors were needed. The partial charges of the inhibitor atoms were taken from electrostatic potential (ESP) calculations fitted to an AM1 wavefunction after an AM1 geometry optimization.[42]

MOE Dock Settings

Using MOE-Dock's graphical interface, a docking box of 70 × 70 × 70 points with a grid spacing of 0.375 Å was centered at −6.8680, 2.6221, 15.9747; 4.258 Å above the zinc atom for CA II. In CA IV, the same docking box was centered at 6.8180, −6.5797, 54.9924; 3.971 Å above the zinc atom. A docking box of this size was used so the ligand could search the entire active site of the enzyme, while the grid spacing was adopted from AutoDock® 2.4. In each trial, the number of runs and cycles was set to 25, while the accept/reject limit was set to 30,000 iterations. The values for runs, cycles, and accept/reject were chosen based on our own trials with AutoDock®, MOE-Dock, and the results of Morris et al.[5] One trial was performed for each inhibitor producing 25 predicted docked structures.

Predicted Docked Structures from MOE

At the completion of each trial, five complexes with the lowest interaction energies (IEs) were chosen and termed the "best" structures. Structures with the same IE, ±1 kcal/mol, were counted as one complex. For example, there can be seven different orientations yet only five different structures due to similar IE values. Structures with the same IE having vastly different geometries were never encountered. All of the predicted structures then were displayed in reference to the active site, His-94, His-96, His-119, threonine 199, and the zinc ion. Knowledge that the sulfonamide group of the inhibitor interacts with the zinc atom of CA is vital and is known through numerous X-ray structures.[23,27] Using this knowledge, structures with an incorrect orientation in the active site, but having low IEs, were discarded. For each of the trials, there were on average one or two of the five possible structures with favorable IE and poor orientation. The remaining structures then were energy minimized. For the majority of the cases, the structure with the lowest or next lowest IE was the overall best-docked structure.

Energy Minimization after Docking

Current docking algorithms do not minimize the receptor after the substrate is docked due to computational cost. Some docking algorithms will perform minimization of the substrate after each docking run. We took the minimizations further by also minimizing the substrate and the active site. Energy minimizations were performed on the "best" predicted docked structures to refine the orientation of the substrate in the receptor site and to find the *local energy minimum* of the inhibitor–enzyme interaction. Using the energy minimization function outlined earlier, two protocols were designed for minimizing the inhibitor–enzyme complexes. In Method 1, the receptor was treated as a rigid structure and the inhibitor was allowed to relax into the active site. For Method 2, the side chains of the active site and the inhibitor were allowed to relax while the rest of the receptor including the backbone of the active site were fixed. Table 2 contains the amino acid and residue number of the CA II and CA IV active site residues that were allowed to relax during Method 2. The energy minimization of the inhibitor in the active site proved useful because the root mean

Table 2. Residue Numbers and Type of Amino Acid Lining the Active Site of CA II and CA IV

	Amino acid			Amino acid	
Residue number	CA II	CA IV	Residue number	CA II	CA IV
7	Tyr	Try	131	Phe	Val
64	His	His	141	Leu	Ile
65	Ala	Ser	143	Val	Val
67	Asn	Met	198	Leu	Leu
91	Ile	Lys	200	Thr	Thr
121	Val	Val	207	Val	Val

squared deviation (RMSD) of the inhibitor—enzyme complex was reduced.

RMSD Calculations and Values

The RMSD value is used as a measure of "how close" the predicted structure was to the X-ray structure of both AMS and AZP bound to CA II and AZP bound to CA IV. RMSD also was used to show the relationship of the change in IE with respect to the overall movement of the inhibitor induced by the minimization methods. RMSD calculations are performed using

$$RMSD = \sqrt{\frac{\Sigma\ (\mathbf{R}_i - \mathbf{R}_i^{ref})^2}{n}}$$

where $\mathbf{R}_i$ are the X, Y, and Z coordinates of the individual atoms of the molecule of interest, $\mathbf{R}_i^{ref}$ are the X, Y, and Z coordinates of the individual atoms of the reference molecule, and n is the number of atoms in the molecule.

RESULTS AND DISCUSSION

Carbonic Anhydrase II

We started with a known sulfonamide–CA complex, AMS bound to CA II. Using MOE-Dock the inhibitor was docked successfully into the active site reproducing the X-ray structure with an RMSD of 1.4Å. There were six "good" predicted structures for the AMS–CA II complex (Color Plate 1). The "best" structure was chosen, based on IE, for further analysis. RMSD values were used to confirm the predicted structures. Starting with this docked structure the RMSD decreased to 1.6 Å after Method 1 and to 1.5 Å after Method 2.

Next we docked AZP into the active site of CA II. The AZP predicted docked structure has an RMSD of 3.8 Å when compared to the X-ray structure.[23] After Method 1 the RMSD value was 3.8 Å and further reduced to 3.7 Å after Method 2. RMSD values for AZP in CA II were calculated without taking into account the aliphatic ether tail because of the large conformational space that it can explore.

The same process was performed on the remaining inhibitors (Color Plate 2). The next step was to compare the IE values to the experimental K_i of Boriack-Sjodin et al. This comparison allowed us to observe the order in which the inhibitors will bind in comparison to each other based on IEs. For CA II the IE values from Method 2 follow the experimental K_i values of Boriack-Sjodin et al.

The images in Color Plate 3 show the hydrogen bonding between the sulfonamide group of AMS and threonine 200 and the hydrogen bond between the hydrogen of the Nϵ2 atom on His-64 and an SO_2 oxygen of AZP. These examples illustrate the importance of hydrogen bonding between a ligand and the active site. This shows that binding of ligands to the active site is not only due to electrostatic interactions, but also by new hydrogen bonding.

Carbonic Anhydrase IV

Comparison of the CA II and CA IV active site revealed some composition differences.[23] The active sites of the isozymes differ by five amino acids, as shown in Table 2. These differences account for the generally decreased affinity of certain sulfonamide inhibitors toward CA IV when compared to CA II and the difference in IEs from MOE-Dock between CA II and IV as shown in Table 3. From the predicted IE values of inhibitors complexed with CA IV, one can anticipate the inhibitor's qualitative binding affinity to be, in order of best to worst: IN2R, IN3R, IN3S, AMS, then AZP (Color Plate 4).

The AZP inhibitor from MOE-Dock had an RMSD of 3.6 Å, from the X-ray structure provided by Stams et al., for both Methods 1 and 2. Again the RMSD values for AZP in CA IV were calculated without taking into account the aliphatic ether tail.

Table 3. Summary of data

	IN3R	AZP	IN2R	IN3S	AMS
CA II					
MOE-Dock energy[a]	−100	−181	−174	−161	−149
MOE interaction energy 1	−258	−271	−267	−266	−233
RMSD from MOE-Dock[b]	1.15	0.61	0.77	0.90	0.60
MOE interaction energy 2	−324	−321	−296	−292	−239
RMSD from MOE-Dock	1.25	0.83	0.52	0.72	0.48
RMSD IE1 structure	0.64	0.64	0.70	0.35	0.32
K_d (nM)	0.10 ± 0.01	0.13 ± 0.03	0.32 ± 0.05	1.70 (single)	750
CA IV					
MOE-Dock energy[a]	−319	−246	−278	−278	−229
MOE interaction energy 1	−287	−163	−343	−232	−291
RMSD from MOE-Dock[b]	0.75	0.65	0.70	0.82	0.49
MOE interaction energy 2	−338	−193	−372	−312	−284
RMSD from MOE-Dock	0.79	0.63	0.70	0.63	0.50
RMSD IE1 structure	0.37	0.15	0.33	0.64	0.11

[a] All interaction energies are in kcal/mol.
[b] All RMSD values are in Å.

SUMMARY

Using a standard protocol it is possible to predict not only the correct orientation of substrates to a specific isozyme, but also the qualitative affinity of a group of substrates for a specific isozyme. Although it is not possible to directly predict the experimental K_i value from IE values, it is possible to qualitatively rank different substrates for a specific enzyme.

Through the use of IE values, one can predict to which isozyme a specific substrate/inhibitor will best bind. In this study, it was known from experimental data that AZP binds better to CA II than CA IV, because the IC_{50} value of 3.2 nM for AZP binding to CA II was compared to 45.3 nM in CA IV.[23] The IE values for AZP binding to CA II versus CA IV are −180 and −246, respectively, for the best predicted docked structures. After Method 1 the IE values are −270 and −163, showing approximately 1.6 times more affinity for CA II over CA IV by AZP. After Method 2 the binding affinity for CA II by AZP had values of −320 and −193 for AZP binding to CA II and CA IV, respectively, again 1.6 times greater binding affinity of AZP toward CA II. Even though the IE values have been determined for the inhibitors in both CA II and CA IV, we are not able to determine the quantitative K_i values (binding affinity). We are only able to qualitatively determine the order of binding affinity for the inhibitors.

ACKNOWLEDGMENTS

We are grateful to the Noble Dick fund at Duquesne University for financial support of this work. The authors would like to thank Dr. Travis Stams for providing the X-ray structure of CA II and CA IV complexed with AZP.

REFERENCES

1 Murcko, M.A. Recent advances in ligand design methods. In: *Computational Chemistry,* Lipkowitz, K.B., and Boyd, D.B., Eds., Wiley-VCH, New York, 1997, Vol. 11, pp. 1–66

2 Trosset, J.-Y., and Scheraga, H.A. Prodock: Software package for protein modeling and docking. *J. Comput. Chem.* 1999, **20,** 412–427

3 Trosset, J.-Y. Flexible docking simulations: Scaled collective variable Monte Carlo minimization approach using Bezier splines, and comparison with a standard Monte Carlo algorithm. *J. Comput. Chem.* 1999, **20,** 244–252

4 Morris, G.M., Goodsell, D.S., Halliday, R.S., Huey, R., Hart, W.E., Belew, R.K., and Olson, A.J. Automated docking using a Lamarckian genetic algorithm and an empirical binding free energy function. *J. Comput. Chem.* 1998, **19,** 1639–1662

5 Morris, G.M., Goodsell, D.S., Huey, R., and Olson, A.J. Distributed automated docking of flexible ligands to proteins: Parallel applications of AutoDock 2.4. *J. Comput. Aided Mol. Des.* 1996, **10,** 293–304

6 Kuntz, I.D. Structure-based strategies for drug design and discovery. *Science* 1992, **257,** 1078–1082

7 Mangoni, M., Roccatano, D., and Nola, A.D. Docking of flexible ligands to flexible receptors in solution by molecular dynamics simulations. *Prot. Struct. Funct. Genet.* 1999, **35,** 153–162

8 Goodsell, D.S., Morris, G.M., and Olson, A.J. Automated docking of flexible ligands: Applications of AutoDock. *J. Mol. Recogn.* 1996, **9,** 1–5

9 Goodsell, D.S., and Olson, A.J. Automated docking of substrates to proteins by simulated annealing. *Prot. Struct. Funct. Genet.* 1990, **8,** 195–202

10 DesJarlais, R.L., Sheridan, R.P. Seibel, G.L., Dixon, J.S., Kuntz, I.D., and Venkataraghavan, R. Using shape complementarity as an initial screen in designing ligands for a receptor binding site of known three-dimensional structure. *J. Med. Chem.* 1988, **31,** 722–729

11 Clark, K.P., and Ajay. Flexible ligand docking without parameter adjustment across four ligand-receptor complexes. *J. Comput. Chem.* 1995, **16,** 1210–1226

12 Apostolakis, J., Plückthun, A., and Caflisch, A. Docking small ligands in flexible binding sites. *J. Comput. Chem.* 1998, **19,** 21–37

13 Vieth, M., Hirst, J.D., Kolinski, A., and Brooks, C.L. III. Assessing energy functions for flexible Docking. *J. Comput. Chem.* 1998, **19,** 1612–1622

14 Vieth, M., Hirst, J.D., Dominy, B.N., Daigler, H., and Brooks, C.L. III. Assessing search strategies for flexible docking. *J. Comput. Chem.* 1998, **19,** 1623–1631

15 Jorgensen, W.L., and Tirado-Rives, J. The OPLS potential function for proteins. Energy minimizations for crystals of cyclic peptides and crambin. *J. Am. Chem. Soc.* 1988, **110,** 1657–1666

16 Halgren, T.A. The Merck force field. I. Basis, form, scope, parameterization, and performace of MMFF94. *J. Comput. Chem.* 1996, **17,** 490–519

17 Brooks, B.R., Bruccoleri, R.E., Olafson, B.D., States, D.J., Swaminathan, D., and Karplus, M. CHARMM: A program for macromolecular energy, minimization, and dynamics calculations. *J. Comput. Chem.* 1983, **4,** 187–217

18 Weiner, S.J., Kollman, P.A., Case, D.A., Singh, C., Ghio, C., Alagona, G., Profeta, S., and Weiner, P. A new force field for molecular mechanical simulation of nucleic acids and proteins. *J. Am. Chem. Soc.* 1984, **106,** 765–784

19 Weiner, S.J., Kollman, P.A., Nguyen, D.T., and Case, D.A. An all atom force field for simulations of proteins and nucleic acids. *J. Comput. Chem.* 1986, **7,** 230–252

20 MacKerell, J., Bashford, D., Bellott, M. Dunbrack, J.R.L., Evanseck, J.D., Field, M.J., Fischer, S. Gao, J., Guo, H., Ha, S., Joseph-McCarthy, D., Kuchnir, L., Kuczera, K., Lau, F.T.K., Mattos, C., Michnick, S., Ngo, T., Nguyen, D.T., Prodhom, B., Reiher, I.W.E., Roux, B., Schlenkrich, M., Smith, J.C., Stote, R., Straub, J., Watanabe, M., Wiorkiewicz-Kuczera, J., Yin, D., and Karplus, M. All-atom empirical potential for molecular modeling and dynamics studies of proteins. *J. Phys. Chem. B* 1998, **102,** 3586–3616

21 Lippard, S.J., and Berg, J.M. *Principles of bioinorganic chemistry.* University Science Books, Mill Valley, CA, 1994, p. 411

22 Boriack-Sjodin, P.A., Zeitlin, S., Chen, H.-H., Crenshaw, L., Gross, S., Dantanarayana, A., Delgado, P., May, J.A., Dean, T., and Christianson, D.W. Structural analysis of inhibitor binding to human carbonic anhydrase II. *Prot. Sci.* 1998, **7,** 2483–2489

23 Stams, T., Chen, Y., Boriack-Sjodin, P.A., Hurt, J.D., Liao, J., May, J.A., Dean, T., Laipis, P., Silverman, D.N., and Christianson, D.W. Structures of murine carbonic anhydrase IV and human carbonic anhydrase II

complexed with brinzolamide: Molecular basis of isozyme-drug discrimination. *Prot. Sci.* 1998, **7,** 556–563
24 Hageman, G.S., Zhu, X.L., Waheed, A., and Sly, W.S. Localization of carbonic anhydrase IV in a specific capillary bed of the human eye. *Proc. Natl. Acad. Sci. USA* 1991, **88,** 2716–2720
25 Baird, T.T. Jr., Waheed, A., Okuyama, T., Sly, W.S., and Fierke, C.A. Catalysis and inhibition of human carbonic anhydrase IV. *Biochemistry* 1997, **36,** 2669–2678
26 Maren, T.H. The general physiology of reactions catalyzed by carbonic anhydrase and their inhibition by sulfonamides. *Ann. N. Y. Acad. Sci.* 1984, **429,** 568–579
27 Boriack, P.A., Christianson, D.W., Kingery-Wood, J., and Whitesides, G.M. Secondary interactions significantly removed from the sulfonamide binding pocket of carbonic anhydrase II influence inhibitor binding constants. *J. Med. Chem.* 1995, **38,** 2286–2291
28 Keilin, D., and Mann, T. Carbonic anhydrase. *Nature* 1939, **144** 442–443
29 Mann, T., and Keilin, D. Sulphanilamide as a specific inhibitor of carbonic anhydrase. *Nature* 1940, **146** 164–165
30 Madura, J.D., Nakajima, Y., Hamilton, R.M., Wierzbicki, A., and Warshel, A. Calculations of the electrostatic free energy contributions to the binding free energy of sulfonamides to carbonic anhydrase. *Struct. Chem.* 1996, **7** 131–138
31 Maren, T.H. Direct measurements of the rate constants of sulfonamides with carbonic anhydrase. *Mol. Pharmacol.* 1992, **41,** 419–426
32 Kernohan, J.C. A method for studying the kinetics of the inhibition of carbonic anhydrase by sulfonamides. *Biochim. Biophys. Acta* 1966, **118,** 405–412
33 Chakravarty, S., and Kannan, K.K. Drug–protein interactions: refined structures of three sulfonamide drug complexes of human anhydrase I enzyme. *J. Mol. Biol.* 1994, **243,** 298–309
34 FTDOCK, 1998, Biomolecular Modeling Laboratory, UK, http://www.bmm.icnet.uk/ftdock/ftdock.html
35 MOE-Dock, 1998.10, 1998, Chemical Computing Group, Inc., Montreal, Quebec, Canada, http://www.chemcomp.com
36 Molecular Operating Environment, 1998.10, 1998, Chemical Computing Group Inc., Montreal, Quebec, Canada, http://www.chemcomp.com
37 Stams, T., Nair, S.K., Okuyama, T., Waheed, A., and Sly, W.S. Crystal structure of the secretory form of membrane-associated human carbonic anhydrase IV at 2.8-Å resolution. *Proc. Natl. Acad. Sci. USA* 1996, **93,** 13589–13594
38 Bernstein, F.C., Koetzle, T.F., Williams, G.J.B., Meyer, E.F. Jr., Brice, M.D., Rodgers, J.R., Kennard, O., Shimanouchi, T., and Tasumi, M. The protein data bank: A computer-based archival file for macromolecular structures. *J. Mol. Biol.* 1977, **112,** 535–542
39 Eriksson, A.E., Jones, T.A., and Liljas, A. Refined structure of human carbonic anhydrase II at 2.0 angstroms resolution. *Prot. Struct. Funct. Genet.* 1988, **4,** 274
40 Gill, P., Murray, W. and Wright, M.H. *Practical optimization.* Academic Press, New York 1981
41 Eriksson, A.E., Kylsten, P.M., Jones, T.A., and Liljas, A. Crystallographic studies of inhibitor binding sites in human carbonic anhydrase II. A pentacoordinated binding of the SCN^- ion to the zinc at high pH. *Prot. Struct. Funct. Genet.* 1988, **4,** 283
42 PC Spartan Pro, 1.0.1, 1999, Wavefunction, Inc., Irvine, California, http://www.wavefun.com

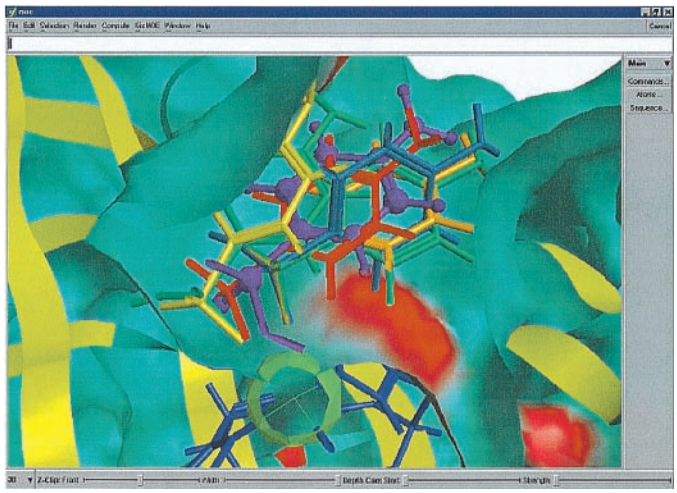

Color Plate 1. The six “best” AMS—CA II MOE-Dock predicted structures. The violet ball-and-stick structure is the AMS X-ray structure.

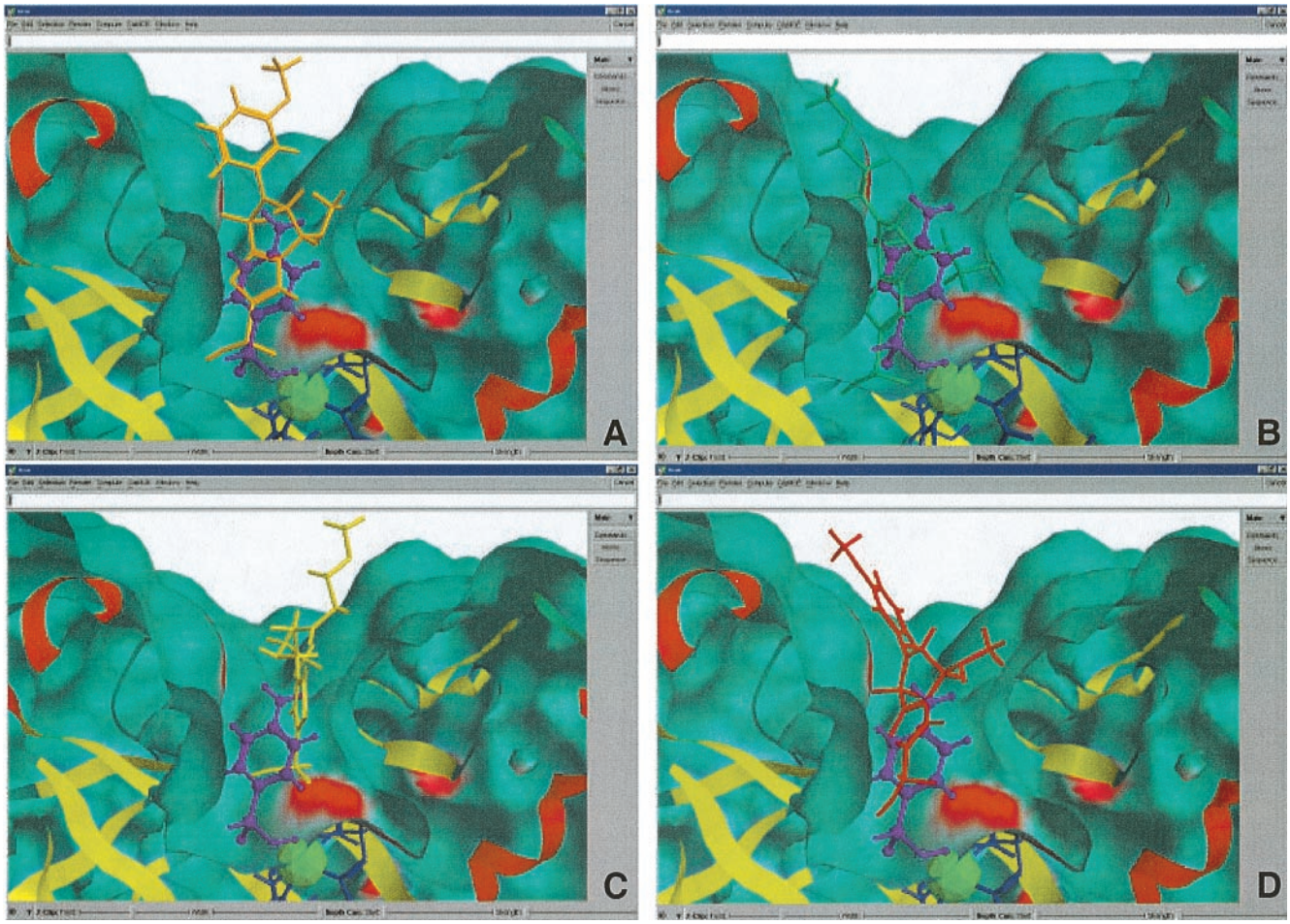

Color Plate 2. The “best” inhibitor–enzyme conformations for the selected CA II inhibitors. The violet ball-and-stick structure is the AMS X-ray structure. (A) IN3R. (B) AZP. (C) IN2R. (D) IN3S.

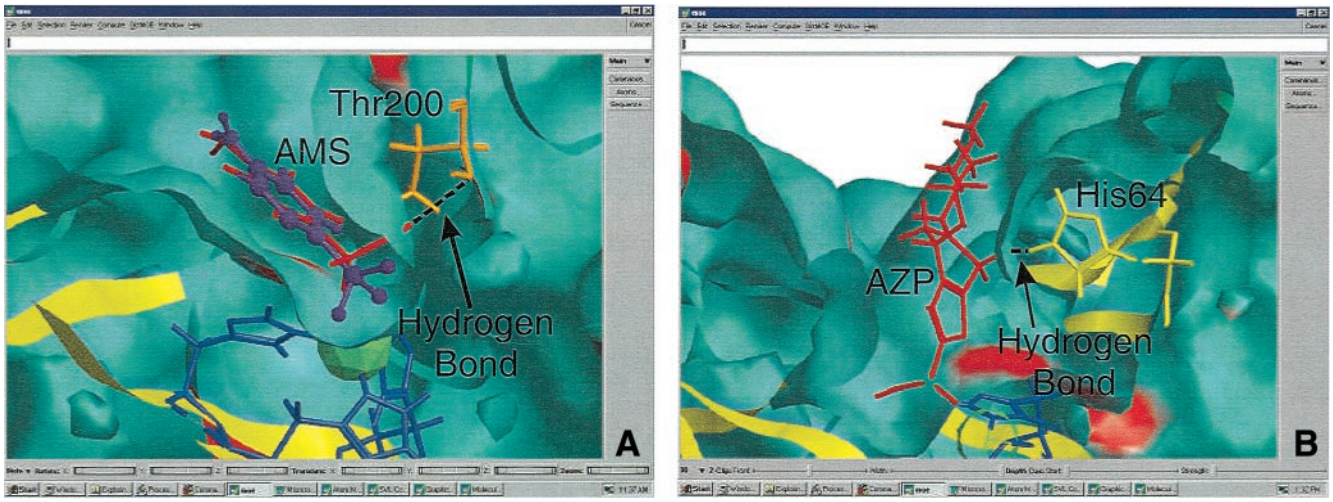

Color Plate 3. Both of these images are of inhibitors interacting with CA II. The top image is the hydrogen bond created between the sulfonamide group of AMS and the nitrogen of Thr200. The violet ball-and-stick structure is the AMS X-ray structure and the red tube structure is the best predicted. The bottom image is the hydrogen bond between the oxygen of the SO_2 group on AZP and the Nε2 hydrogen on His-64.

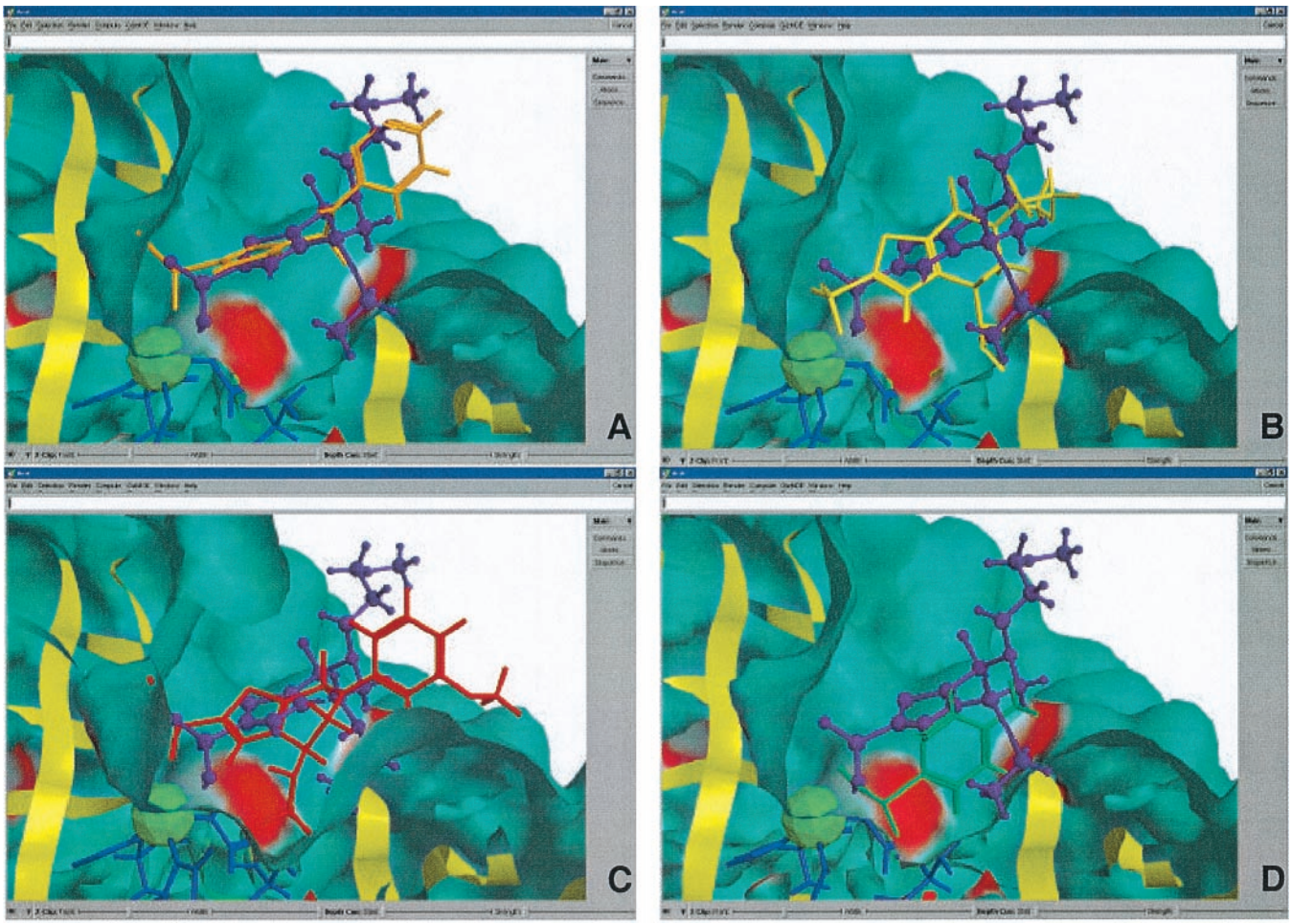

Color Plate 4. The "best" CA IV inhibitor–enzyme conformations. The violet ball-and-stick structure is the AZP X-ray structure provided by Stams et al. (A) IN3R. (B) IN2R. (C) IN3S. (D) AMS.